

## Measurement of electro-magnetic radiation at PHENIX

Takao Sakaguchi for the PHENIX Collaboration

<sup>1</sup> Brookhaven National Laboratory, Physics Department,  
Upton, NY 11973-5000, U.S.A.

**Abstract.** Recent results on direct photons and dileptons from the PHENIX experiment opened up a possibility of landscaping electro-magnetic radiation over various kinetic energies in heavy ion collisions. A detail discussion is given based on a review of the results.

*Keywords:* direct photons, dileptons, Au+Au, p+p, RHIC, PHENIX, QGP, pQCD

*PACS:* 12.38.Mh, 12.38.-t, 24.85.+p, 25.75.Nq

### 1. Introduction

Electro-magnetic radiation is an excellent probe for extracting thermodynamical information. They are emitted from all the stages of collisions, and don't interact strongly with medium once produced. Therefore, many heavy ion experiments have explored the radiation. As stated in several literatures [ 1, 2], the electro-magnetic radiation stands for a direct radiation from the matter produced or a prompt reaction such as initial hard scattering. In this sense,  $\pi^0$ ,  $\eta$ ,  $\rho$ ,  $\omega$  or  $\phi$  mesons decaying into photons or leptons are not defined as electro-magnetic radiations.

The electro-magnetic radiation is primarily produced through a Compton scattering of quarks and gluons ( $qg \rightarrow q\gamma$ ) and an annihilation of quarks and anti-quarks ( $q\bar{q} \rightarrow g\gamma$ ) as leading order processes, and the next leading process is dominated by bremsstrahlung (fragment) ( $qg \rightarrow qq\gamma$ ). There is also a prediction of a jet-photon conversion process, which occurs if a QGP is formed, by a secondary interaction of a hard scattered parton with thermal partons in the medium [ 3, 4].

A calculation predicts that a photon contribution from the QGP state is predominant in the  $p_T$  range of  $1 < p_T < 3 \text{ GeV}/c$  [ 5]. The signal is usually seen after subtracting photons from known hadronic sources. The typical signal to background ratio is  $\sim 10\%$ . For  $p_T > 3 \text{ GeV}/c$ , the signal is dominated by a contribution from initial hard scattering, and  $p_T < 1 \text{ GeV}$ , the signal is from hadron gas through processes of  $\pi\pi(\rho) \rightarrow \gamma\rho(\pi)$ ,  $\pi K^* \rightarrow K\gamma$  and etc..

One of the big successes by now in electro-magnetic radiation measurement is the observation of high  $p_T$  direct photons that are produced in initial hard scattering [ 2]. The high  $p_T$  hadron suppression found at RHIC is interpreted as a consequence of an energy loss of hard-scattered partons in the hot and dense medium. It was strongly supported by the fact that the high  $p_T$  direct photons are not suppressed and well described by a NLO pQCD calculation.

Photons are converted into virtual photons with a certain probability via internal conversion process (e.g.  $q\bar{q} \rightarrow q\gamma \rightarrow q\gamma^* \rightarrow ql^+l^-$ ). This fact opened up various approaches of looking at "photons" over a broad range of energies in a mid-rapidity; for low energy "photons" ( $E < 1$  GeV), photons can be measured via low mass and low  $p_T$  dileptons (virtual photons) that decay into electrons. High energy photons ( $E > 5$  GeV) can be measured as themselves with an electro magnetic calorimeter. In the intermediate energy region ( $1 < E < 5$  GeV), both dileptons and real photons can be measured, and helps disentangling various contributions. The idea is illustrated in Fig. 1.

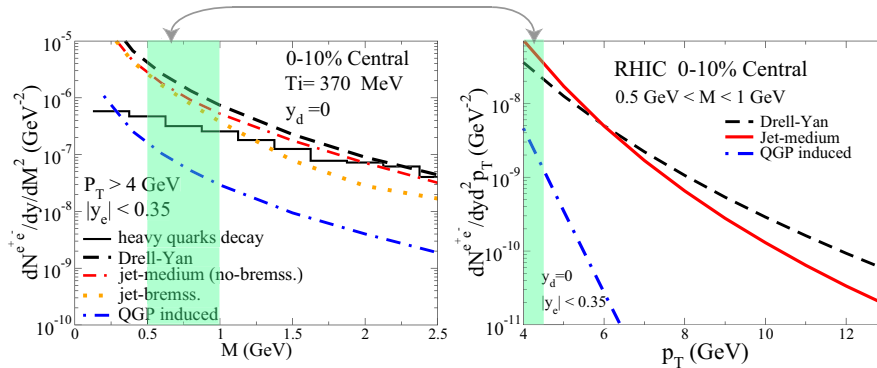


**Fig. 1.** Prediction of dilepton yields at high mass and low  $p_T$ , and low mass and high  $p_T$  [ 6]. The shaded bands show similar kinetic regions, and one can disentangle contributions by comparing the yields.

In this paper, electro-magnetic radiation is landscaped by reviewing the latest results on direct photon and dileptons from the PHENIX experiment.

## 2. Dilepton (di-electron) measurement

Dileptons (di-electrons) have been measured at the PHENIX experiment using the high statistics Au+Au data in Year-4 [ 7, 8]. Electrons are tracked by a drift chamber with an excellent momentum resolution. A Cherenkov counter in the PHENIX experiment that has a hadron rejection power on  $10^4$  for a single track separates electrons from  $\pi^{+/-}$  well up to 4.9 GeV/c. The Fig. 2(a) shows the dilepton mass spectra for  $\sim 700$  M minimum bias Au+Au events. The  $p_T$  cut of 0.3 GeV/c is applied for single electrons. The ratios of several mass ranges are shown in Figs. 2(b) and (c). The mass region of 0-100 MeV/c<sup>2</sup> represents mainly a contribution from

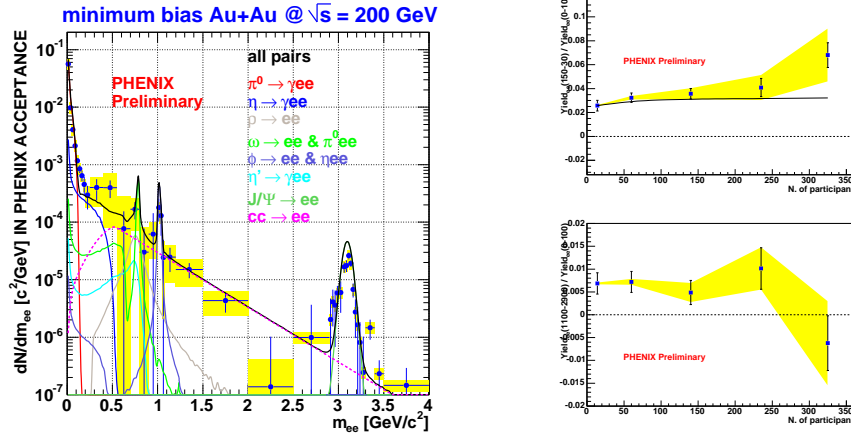


**Fig. 2.** (a) Invariant mass distribution of dileptons with cocktail calculation from hadron decays (left). Ratios of yields in (b) 150-300 MeV/ $c^2$  (right top) and (c) 1.1-2.9 GeV/ $c^2$  (right bottom) to that in 0-100 MeV/ $c^2$ , as a function of centrality.

$\pi^0$ 's. In Fig. 2(b), the ratio of the yields in 150-300 MeV/ $c^2$  to 0-100 MeV/ $c^2$  is shown with the one from known hadron decay contribution as a line. Although the systematic error is large, there is an excess in most central collisions. This mass region corresponds to the kinematic region where hadron-gas interaction plays a main role.

In Fig. 2(c), the ratio of yields in 1.1-2.9 GeV/ $c^2$  to 0-100 MeV/ $c^2$  is shown. The ratio stays a constant up to mid-central and drops in the most central collisions. In order to investigate the source of contributions in the mass region, a nuclear modification factor ( $R_{AA}$ ) for the yield in the mass region was calculated and compared with those for single electrons and  $\pi^0$ 's (Fig. 3). For dileptons, the  $R_{cp}$  (central to peripheral yield ratio) is plotted instead of  $R_{AA}$  because there is no reference data from p+p collisions. The result shows that the yield follows the suppression pattern of single electrons and  $\pi^0$ 's that mainly come from semi-leptonic decay of charm quarks and jets, respectively. The suppression of intermediate mass dileptons could attribute to an energy loss of charm quarks, but may also be related to alteration of an opening angle of two electrons coming from back-to-back  $c\bar{c}$  pairs. The thermal radiation is also expected to exist in this region, but is not clearly seen with current errors.

### 3. Direct photon measurement

Direct photons are measured in Au+Au collisions at  $\sqrt{s_{NN}}=200$  GeV, and p+p collisions at  $\sqrt{s}=200$  GeV as shown in Figs. 4 [9]. The direct photons in p+p collisions are measured up to 25 GeV/ $c$ , and can be used as a reference for quantifying a medium effect in Au+Au collisions. The data is compared with a NLO pQCD

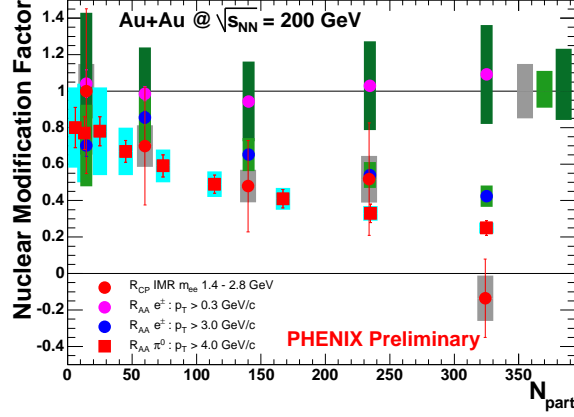


**Fig. 3.** Nuclear Modification factor ( $R_{AA}$ ) for intermediate mass region (1.4-2.8 GeV/ $c^2$ ) compared with those for single electrons ( $p_T > 0.3$  GeV/ $c$  and  $p_T > 2.0$  GeV/ $c$ ) and  $\pi^0$ s. Note that  $R_{cp}$  (central to peripheral yield ratio) is plotted for dileptons.

calculation [11], and found that it is well described by the calculation within  $\sim 40\%$  down to 5 GeV/ $c$ . Since the  $p_T$  binning is different between Au+Au and p+p re-

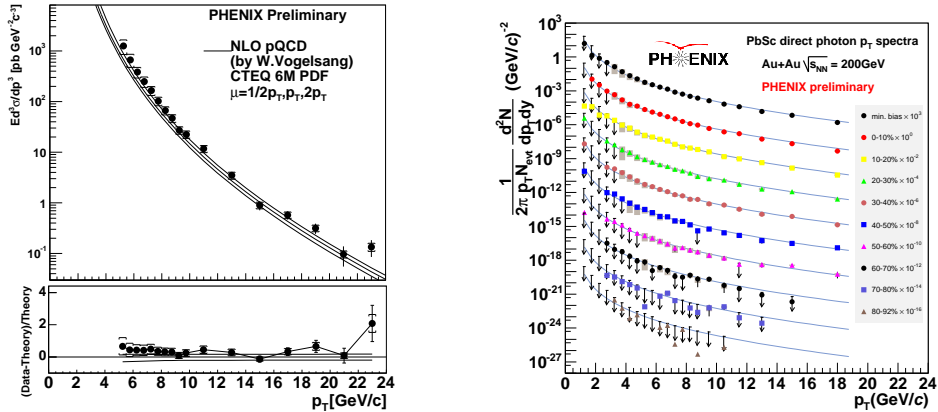


**Fig. 4.** (a) Direct photon results in Au+Au collisions at  $\sqrt{s_{NN}}=200$  GeV (left) and (b) in p+p collisions at  $\sqrt{s}=200$  GeV (right).

sults, the p+p data is fitted with a power-law function to interpolate the  $p_T$  points of Au+Au data. The fit describes the data very well within  $\sim 5\%$ . Fig 5 shows the  $R_{AA}$  of direct photons in Au+Au collisions. In Year-2 data, we were not able to reach above 12 GeV/ $c$ , where the  $R_{AA}$  was consistent with unity, and thus concluded that direct photons are unmodified by the medium. The latest data shows a trend of decreasing at high  $p_T$  ( $p_T > 14$  GeV/ $c$ ).

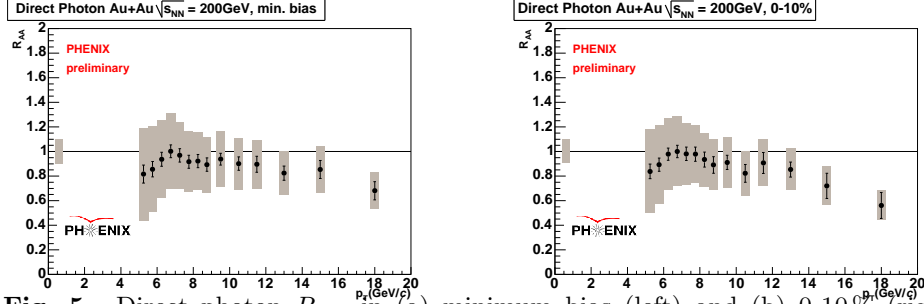


**Fig. 5.** Direct photon  $R_{AA}$  in (a) minimum bias (left) and (b) 0-10% (right) Au+Au collisions at  $\sqrt{s_{NN}}=200$  GeV.

There are several implications of the data such as suppression of fragment photons (30% of total NLO pQCD photons at 14 GeV/c, and decreases as  $p_T$  increases.) due to an energy loss of quarks, or an isospin effect [12]. Here, simple models are proposed to understand the result [10]. The major contribution to direct photon production at the  $p_T$  range of the interest is from Compton scattering process ( $qg \rightarrow q\gamma$ ), therefore, we can assume that the yield is naively described as:

$$Yield(x_T, Q^2) = F_{2p}(x_T) \times g_p(x_T) \times \sigma^{dir.\gamma}(x_T, Q^2)$$

where  $F_{2p}$  is the quark parton distribution function (PDF), and  $g_p$  is the gluon PDF. The  $R_{AA}$  can be written as:

$$R_{AA} = \frac{d^2\sigma_{\gamma}^{AA}/dp_T^2 dy}{AA d^2\sigma_{\gamma}^{pp}/dp_T^2 dy} \approx \left( \frac{F_{2A}(x_T)}{AF_{2p}(x_T)} \times \frac{g_A(x_T)}{Ag_p(x_T)} \right)$$

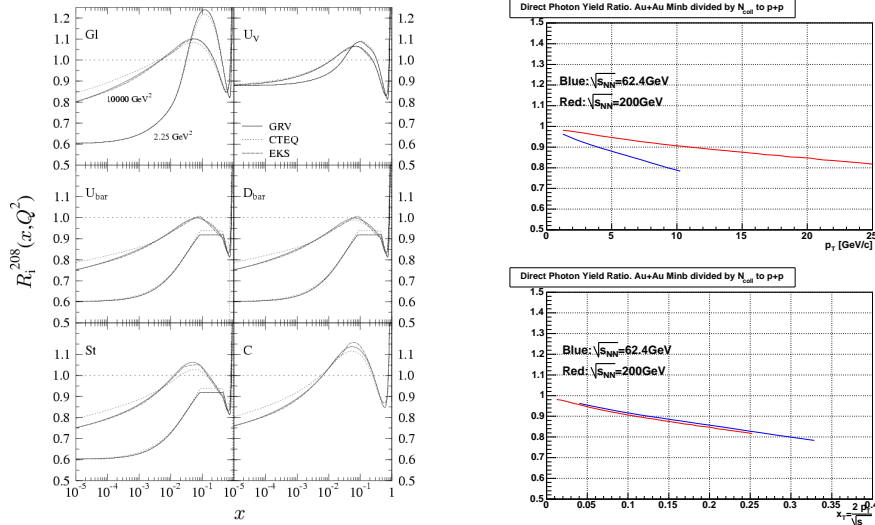
The PDFs are shown in Fig. 6(a) [13]. The decrease of the yield in Au+Au starts at  $\sim 12$  GeV/c and drop by  $\sim 30\%$  at 18 GeV/c, which corresponds to  $x = 0.12$  to 0.18. Just from the parton distribution function, it seems that the significant drop of  $R_{AA}$  at high  $p_T$  is not well explained. The structure function can be measured in a future high statistics d+Au collisions.

The isospin effect is an effect caused from the difference of the quark charge contents in neutrons and protons. The photon production cross-section is proportional to  $\alpha\alpha_s \sum e_q^2$ , therefore the yield of photons will be different between n+p, p+p and n+n collisions [11]. A gold ion consists of 79 protons and 118 neutrons. We can calculate the hard scattering cross-section for minimum bias Au+Au collisions by weighting those for n+p, p+p and n+n as follows:

$$\frac{\sigma_{AA}}{\langle N_{coll} \rangle} = \frac{1}{A^2} \times (Z^2\sigma_{pp} + 2Z(A-Z)\sigma_{pn} + (A-Z)^2\sigma_{nn})$$

The  $R_{AA}$  expected from isospin effect can be calculated as:

$$R_{AA} = \frac{\sigma_{AA}}{\langle N_{coll} \rangle \sigma_{pp}}$$



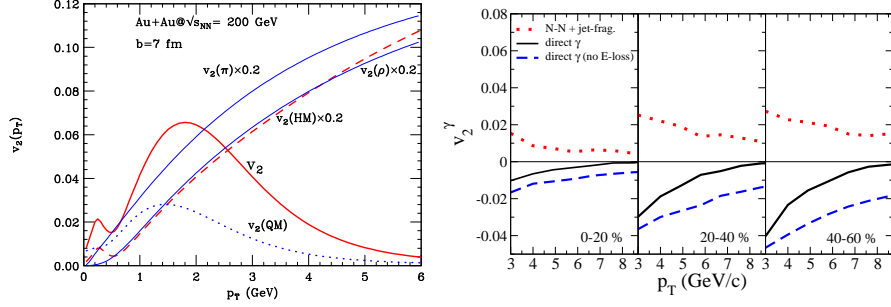
**Fig. 6.** (a) Parton distribution functions and (b) expected isospin effect in Au+Au collisions calculated from n+p, p+p and n+n direct photon cross-sections.

Fig. 6(b) shows the  $R_{AA}$  calculated in this way. The calculation at  $\sqrt{s_{NN}}=200\text{GeV}$  is shown in red. There is  $\sim 15\%$  drop at  $18\text{GeV}/c$  caused by the effect. If we combine the structure function effect with the isospin effect, the data could be explained. It also means that the direct photons may not be modified by a medium as expected. For a reference, the one at  $\sqrt{s_{NN}}=62.4\text{GeV}$  is also shown as blue. It is seen that the suppression is larger at the energy because the effect scales with  $x_T$  as shown in the bottom of Fig. 6(b). The calculation suggests that by looking at a  $62.4\text{GeV}$  result, we can quantify the isospin effect in Au+Au collisions. The analysis is ongoing.

#### 4. Direct photon $v_2$

The contribution of photons can be disentangled by looking at the yield as a function of their emission angles with refer to a reaction plane. Figs 7 show predictions of elliptic flow depending on emission sources [ 14, 15]. The flow of photons from hadron-gas interaction and thermal radiation follows the collective expansion of a system, and would give a positive  $v_2$ . The yield of photons produced by a Compton scattering of hard scattered partons and medium thermal partons (jet-photon conversion) increases as the thickness of the matter to traverse increases, and thus gives a negative  $v_2$ . The bremsstrahlung photons will also increase in out-plane, and gives a negative  $v_2$ . The intrinsic fragment or bremsstrahlung photons from jets will be increased in in-plane, since a larger energy loss of jets in out-plane will result in a lower yield of photons originated from the jet at a given  $p_T$ .

PHENIX has measured the  $v_2$  of direct photons by subtracting the  $v_2$  of hadron



**Fig. 7.** Predictions of elliptic flow of thermal (hadronic gas and partonic state) photons (left), and jet-photon conversion, Bremsstrahlung and initial hard scattering photons (right).

decay photons from that of inclusive photons as follows:

$$v_2^{dir.} = \frac{v_2^{incl.} - v_2^{bkgd.}}{R - 1}$$

where

$$R = \frac{(\gamma/\pi^0)_{meas}}{(\gamma/\pi^0)_{bkgd}}$$

comes from the spectral analysis [ 9]. The result is shown in Figs. 8 [ 16]. Although the systematic error is very large, the  $v_2$  of direct photons tend to be positive in 3-6 GeV/c independent of centrality, which is opposed to the predictions. The reduction of the systematic errors is now ongoing to make the final conclusion.

## 5. Conclusions

Recent results on direct photons and dileptons from the PHENIX experiment opened up a possibility of landscaping electro-magnetic radiation over various kinetic energies in heavy ion collisions. A detail discussion is given based on a review of the results. The direct photon result in 62.4 GeV Au+Au collisions will disentangle the effect involved at high  $p_T$ .

## References

1. G. Agakichiev et al., (CERES Coll.), *Eur. Phys. J* **C41** (2005)475.
2. S.S. Adler et al. (PHENIX Coll.), *Phys. Rev. Lett.* **94**, 232301(2005).
3. C. Gale, *Nucl. Phys.* **A785**(2007)93.
4. R. Fries et al., *Phys. Rev.* **C72**, 041902(2005).
5. S. Turbide, R. Rapp and C. Gale, *Phys. Rev.* **C69**, 140903 (2004).

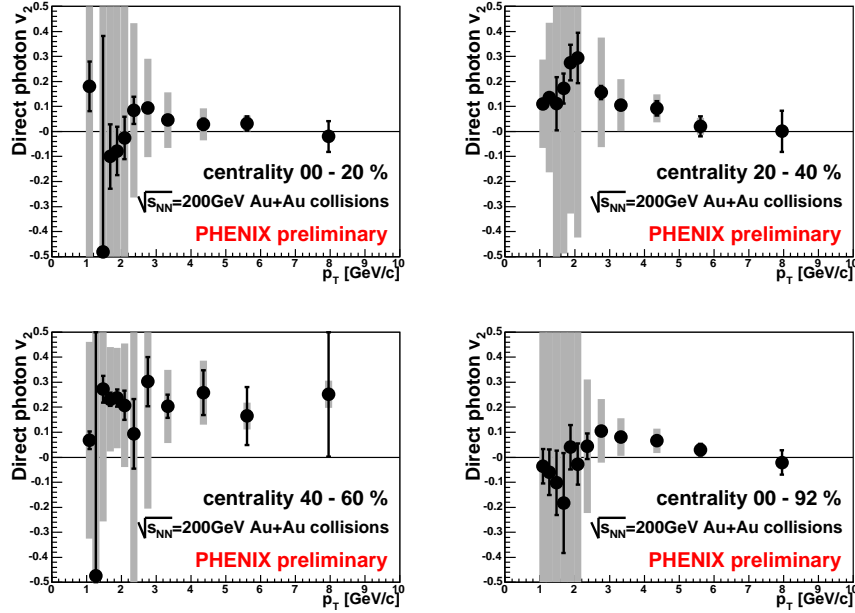


Fig. 8. Elliptic flow of direct photons in Au+Au collisions at  $\sqrt{s_{NN}}=200$  GeV.

6. S. Turbide and C. Gale, *hep-ph/0701230*.
7. A. Toia (PHENIX Coll.), *Nucl. Phys.* **A774**(2006)743.
8. S. Campbell (PHENIX Coll.), to be published in QM2006 Proc.
9. T. Isobe (PHENIX Coll.), *nucl-ex/0701040*.
10. priv. comm. with Michael J. Tannenbaum.
11. L.E. Gordon and W. Vogelsang, *Phys. Rev.* **D48**, 3136 (1993); priv. comm.
12. F. Arleo, *JHEP* **0609**(2006)015.
13. K.J. Eskola, V.J. Kolhinen and C.A. Salgado, *Eur. Phys. J* **C9**(1999)61
14. S. Turbide et al., *Phys. Rev. Lett.* **96**, 032303(2006).
15. R. Chatterjee et al., *Phys. Rev. Lett.* **96**, 202302(2006).
16. K. Miki (PHENIX Coll.), to be published in QM2006 Proc.